Biomass and Bioenergy 203 (2025) 108320

Contents lists available at ScienceDirect

Biomass and Bioenergy

journal homepage: www.elsevier.com/locate/biombioe

Enhanced catalytic conversion of cellobiose/cellulose to 5-hydroxymethylfurfural using dual catalysts: Sulfonated activated carbon and Lewis acid catalyst

Richa Tomer [a,b], Alessia Tonelli [a], Anthony Morena [c], Luca Fusaro [c], Vera Meynen [b], Carmela Aprile [c], Sophie Hermans [a,*]

[a] IMCN Institute, MOST Division, Université Catholique de Louvain (UCLouvain), Place L. Pasteur 1, 1348, Louvain-la-Neuve, Belgium
[b] Laboratory of Adsorption and Catalysis (LADCA), University of Antwerp, Groenenborgerlaan 171, 2020 Antwerpen, Belgium
[c] University of Namur, NISM, Department of Chemistry, Unit of Nanomaterials Chemistry, 5000 Namur, Belgium

ARTICLE INFO

Keywords:
Sulfonic groups
B/L ratio
5-Hydroxymethylfurfural
Isolation
Cellulose

ABSTRACT

An activated carbon (SX+) was functionalized with sulfonic groups via the diazonium coupling method to impart Brönsted (B) acidity to catalyze cellobiose and cellulose upgrading into 5-HMF. X-ray photoelectron spectroscopy (XPS) confirmed SO_3H groups grafting, which significantly enhanced the total acidity to 1.33 mmol/g cat., as confirmed by Boehm titration. The B nature of acidity was verified by ^{31}P ssNMR. The catalytic activity of SO_3H/SX+ alone and with $AlCl_3$ as Lewis (L) acid was evaluated by optimizing reaction conditions such as temperature, solvent, and B/L ratio. A ~47 % 5-HMF yield was obtained with 100 % cellobiose conversion at 150 °C, 4 h with SO_3H/Al ratio of 1:10 in Milli-Q water (MQ)/tetrahydrofuran (THF) solvent. When $AlCl_3$ was replaced with heterogeneous Lewis acidic catalysts (γ-Al_2O_3, AlOOH, and TiO_2), TiO_2 combined with SO_3H/SX+ showed similar catalytic activity, achieving ~50 % yield of 5-HMF with 100 % cellobiose conversion, attributed to its high total acidity (2.4×10^{-2} mol/g cat.). 5-HMF was isolated from the reaction mixture using liquid-liquid extraction, resulting in ~98 % pure 5-HMF. Moreover, SO_3H/SX+ efficiently cleaved the glycosidic bonds of microcrystalline cellulose by giving a ~24 % 5-HMF yield when combined with Lewis acid TiO_2. This study presents a novel dual catalytic system, utilizing an optimized B/L acidity ratio to achieve efficient cellulose conversion into 5-HMF.

1. Introduction

Upgrading and valorizing the lignocellulosic biomass (LCB) into high-value chemicals and fuels is under intense study, due to the depletion of fossil resources and their carbon footprint. LCB can be a potential resource to replace fossil sources due to its abundance, environmental friendliness, and affordability [1]. It is a rich source of polysaccharides, the main one being cellulose, a polymer of D-glucose. Among the valuable products derived from cellulose, 5-hydroxymethylfurfural (5-HMF) has gained significant attention. This versatile compound can be widely used across various industries, including as a starting reagent for pharmaceuticals, polymers, paints, food and flavor, fine chemicals, biofuels, and agrochemicals [2]. That is why it comes in a list of the most important renewable building block chemicals [3]. It can be produced from cellulose by following a cascade of reactions (Fig. 1), i.e. hydrolysis of cellulose to glucose, isomerization of glucose to fructose, dehydration of fructose to 5-HMF, that can be followed by rehydration of 5-HMF to levulinic acid (LA) and Formic acid (FA), in the presence of Brönsted (B) and Lewis (L) acid catalysts [4,5]. Hence, the ratio between B and L sites plays a key role in achieving selective cellulose conversion to 5-HMF, together with optimization of reaction conditions, such as temperature, time, feedstock composition, and reaction solvents.

In an attempt to achieve higher yields of 5-HMF, numerous prior studies have focused on the dehydration of cellulose, glucose, or fructose to 5-HMF. Most reports concentrate on glucose/fructose dehydration, reporting high 5-HMF yields (60–90 %) [6–8], while lower yields (<50 %) [9,10] under a temperature range of 120–200 °C, are generally observed for cellulose due to its stubborn crystalline structure and depolymerization challenges [11,12]. Various catalysts such as

* Corresponding author.
E-mail address: sophie.hermans@uclouvain.be (S. Hermans).

https://doi.org/10.1016/j.biombioe.2025.108320
Received 30 May 2025; Received in revised form 30 July 2025; Accepted 24 August 2025
Available online 5 September 2025

sulfated/phosphated transition metals [6,13], metal-organic frameworks (MOFs) [14,15], zeolites [16–18], and carbon-based materials [19–22] have been developed to ensure the economic sustainability of large-scale 5-HMF production. Among these, carbon-based catalysts have attracted significant attention due to their advantageous properties, including high surface area (800–1200 m^2/g), tunable surface functionality, abundance, low cost (which can be as low as 1 USD/kg), renewability, and environmental friendliness [23,24]. Multiple reports have been published on 5-HMF production, particularly from glucose and fructose, using carbon-based catalysts [15,20–22,25–28]. For example, L. Yan (2014) [25] modified a corn stalk-derived carbonaceous solid acid catalyst with concentrated sulfuric acid and achieved a 5-HMF yield of 44.1 % via the one-step conversion of corn stalk, as a glucose source, in the [BMIM][Cl] ionic liquid at 150 °C in 30 min. However, the use of ionic liquids is not industrially attractive. Niobia/carbon composites (Nb/C) were synthesized and tested for the cellulose hydrolysis reaction by X. Li (2018) [21]. In a THF/H_2O biphasic system, an HMF yield of 53.3 % was reported from cellulose after 8 h of reaction at 170 °C [21]. Q. Wu (2019) [22] synthesized nickel-doped porous carbon material (Ni/CS) with varying percentages of nickel and achieved an 85 % yield of 5-HMF from cellulose using hydrogen (6 MPa) at 200 °C for 60 min, with 200 mg of the $Ni_{2.0}$/CS catalyst. The addition of Ni increased the concentration of O-based acidic groups on CS, because of the nature of the Ni precursor (nickel acetate) used, which in the final catalyst enhanced the B acidity. Das (2022) [26] used red mud, coated it with carbon from glucose, and further modified it with sulfuric acid, achieving a 5-HMF yield of 51.5 % with 93 % glucose conversion in DMSO/water at 180 °C in 30 min under microwave heating. Tempelman (2023) [28] synthesized tin-doped sulfonated activated carbon (Sn-Fn-AC) catalysts and evaluated them on a sugar mixture (glucose + fructose + sucrose), a model of apple pomace, in a water/MIBK (methyl isobutyl ketone) solvent system, reporting a 30 % 5-HMF yield in 80 min at 120 °C. Sien Yan (2024) [19] developed a lignin-derived carbon--supported tin oxide (SnOx/LC-500) catalyst, reporting a 5-HMF yield of 50.1 % from glucose at 190 °C after 3 h in a water-NaCl/THF medium. Several studies have been reported on carbon-based materials for 5-HMF production as illustrated above, however, understanding the reaction conditions such as the Brönsted to Lewis acidity (B/L) ratio or solvent choice, to reach higher 5-HMF yields, are still critical to further enhance yields and reaction conditions, which are important for industrial-scale production of 5-HMF. Moreover, the separation and purification of 5-HMF are other aspects that still need further development [29,30].

Hence, in this study, we aim to thoroughly investigate the effect of the B/L ratio using both homogeneous and heterogeneous Lewis acid catalysts along with our synthesized sulfonic acid-functionalized activated carbon (SO_3H/SX+), which serves as a strong Brönsted acid source for the hydrolysis of cellobiose. The catalyst and reaction conditions were evaluated on cellobiose, a soluble model molecule for raw cellulose, and also tested on cellulose fibers (medium size) with the optimized system. The sulfonic acid groups were covalently grafted on activated carbon using a diazonium coupling method, and the catalyst was characterized by XPS, N_2-physisorption, TGA, Boehm titration and ^{31}P ssNMR. We then explored the key reaction parameters, including reaction temperature (120–150 °C), reaction media (Milli-Q water (MQ), MQ/tetrahydrofuran (THF), MQ-NaCl/THF), and B/L ratios in the presence of $AlCl_3$ as a homogeneous Lewis acid in combination with the SO_3H/SX + solid material. Subsequently, the homogeneous $AlCl_3$ was replaced by heterogeneous Lewis acid catalysts, including Al_2O_3, AlOOH, and TiO_2. Moreover, the isolation of the final product, i.e. 5-HMF, from the reaction mixture was carried out using the liquid-liquid extraction technique to reach high purity. Finally, sulfonic groups grafted activated carbon in combination with TiO_2 were also tested for non-soluble cellulose conversion to 5-HMF at the optimized reaction conditions. Therefore, this study might provide valuable insights into optimizing the tunable Brönsted and Lewis acidity ratios for catalyst synthesis that can help in selectively achieving the highest possible yield of 5-HMF via cellobiose or cellulose upgrading, in a sustainable chemistry context.

2. Experimental

2.1. Synthesis of carbon Brönsted acid catalyst

The activated carbon (SX+) functionalized with sulfonic acid groups was prepared by following the diazonium coupling reaction as reported in our previous work [31,32]. In the classical synthesis method, 1 g of activated carbon (SX+) (NORIT) was homogeneously dispersed in 60 mL of distilled water, followed by the addition of 1.5 g of sulfalinic acid (99 %, Sigma Aldrich) at 70 °C for 10 min for a complete dissolution. Further, the obtained mixture was cooled down to 30 °C, followed by slow addition of 1.2 mL of isopentyl nitrite (96 %, Sigma Aldrich) while stirring. The reaction mixture was kept on stirring for another 16 h, followed by filtering out the solid and washing it with distilled water and ethanol. The obtained powder was dried at 100 °C overnight (16 h) in a conventional oven. The obtained dried black powder was labelled SO_3H/SX+.

2.2. Synthesis of heterogeneous Lewis acidic catalysts

2.2.1. γ-Al_2O_3

A commercially available γ-Al_2O_3 powder from Alfa Aesar (99.97 %, Germany) with a surface area of 80–120 m^2/g and 3 μm APS (average particle size) was used as a heterogeneous Lewis acidity source.

2.2.2. Boehmite (AlOOH)

Boehmite (AlOOH) was hydrothermally prepared by following the method reported by Z. Tang (2019) [33]. In a typical synthesis, a solution of 0.75 M (2.37 g in 40 mL water) of ammonium bicarbonate (≥99.0 %, Sigma Aldrich) was gradually added to 1.5 M (5.63 g in 10 mL water) aluminum nitrate nonahydrate (99.99 %, Sigma Aldrich) under continuous stirring (800–1000 rpm). Further, the pH of the solution of the obtained mixture was adjusted to 9 by dropwise addition of a 25 % aqueous ammonia solution (a few drops). The resulting mixture was then transferred into a 100 mL Teflon-lined stainless-steel autoclave, securely sealed, and heated overnight (16 h) at 150 °C in a conventional oven. Subsequently, the autoclave was allowed to cool naturally to room temperature. The solid product was separated by centrifugation at 6000 rpm for 30 min, followed by washing three times with deionized water. The wet material was then vacuum dried at 80 °C for 24 h. The obtained white material was ground via mortar and pestle and designated as AlOOH catalyst.

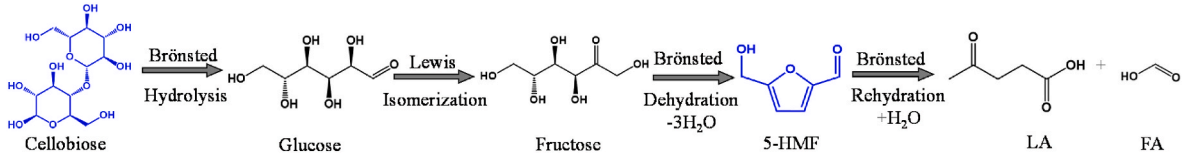

Fig. 1. Typical reaction pathway of cellobiose hydrolysis to 5-HMF production (cellobiose is the simplest disaccharide used as a soluble model for cellulose, which is a polymer of glucose units.).

2.2.3. TiO_2

The TiO_2 heterogeneous Lewis catalyst was synthesized using the sol-gel hydrolysis method, as previously reported by us [7]. In brief, 20 mL of tetraisopropyl orthotitanate (≥98 %, Sigma Aldrich) was mixed with 40 mL of 2-propanol and stirred for 5 min to achieve a homogeneous solution. Distilled water (80 mL) was then added dropwise to this solution to initiate hydrolysis, followed by stirring for 2 h. Further, 100 mL of 0.5 M HCl (37 %, VWR Chemicals) was slowly added to the above mixture to ensure complete hydrolysis of titanium isopropoxide. After 3 h of stirring, the mixture was aged overnight at room temperature without stirring. The next morning, the resulting white slurry was repeatedly diluted and decanted with deionized water until the pH of the solution reached approximately 2–3. The white suspension was kept in a conventional oven at 70 °C for 3 h to obtain a gel, which was then dried overnight (16 h) at 120 °C in the oven. The obtained shiny white agglomerated particles were ground via mortar pestle and calcined at 200 °C for 2 h in a muffle furnace with a heating ramp of 10 °C per min under an air atmosphere. The obtained solid white catalyst was denoted as TiO_2.

2.3. Catalysts characterizations

The synthesized materials were characterized by X-ray photoelectron spectroscopy (XPS), N_2-physisorption, scanning electron microscope, CHNS analysis, thermogravimetric analysis (TGA), powder X-ray diffraction (XRD), ammonia temperature-programmed desorption (NH_3-TPD), Boehm titration techniques and ^{31}P solid-state nuclear magnetic resonance (ssNMR).

XPS analyses were conducted at ambient temperature utilizing an SSX 100/206 spectrometer from Surface Science Instruments (USA). This system includes a monochromatized microfocus aluminium X-ray source. The samples were affixed to small holders using double-sided adhesive tape and positioned on an insulating ceramic carousel (Macor®, Switzerland). To prevent charge build-up, a nickel grid was placed above the samples, and a flood gun set to 8 eV was employed. Binding energies were referenced to the C-(C, H) component of the C1s peak, which was set at 284.4 eV. Data processing was conducted with the CasaXPS software (Casa Software Ltd., UK). The peaks were decomposed into a sum of Gaussian/Lorentzian (85/15) after subtraction of a Shirley-type baseline, using sensitivity factors provided by the manufacturer. The integration of the peaks yielded results in at.% for each element, allowing the calculation of elemental surface ratios in at.%/at.%. The analytical accuracy of the performed XPS probing is ±10 %.

The specific surface area of the synthesized catalysts was measured using the nitrogen physisorption method with a Micromeritics Instruments apparatus from the USA (Model: ASAP 2020). Before analysis, the samples underwent degassing at 150 °C for 10 h under vacuum. The Brunauer-Emmett-Teller (BET) equation was applied to determine the surface area, and the Barrett-Joyner-Halenda (BJH) method was used to assess the pore size distribution of the catalysts from a pore size of 5 Å for both materials.

SEM images were obtained on a JEOL 7600F Field-Emission Scanning Electron Microscope operating at 15.0 kV. The samples were prepared by placing the powders on a double-faced copper tape supported on a thin aluminium lamina. The applied probe current was set at 12 A for direct imaging on powders, and at 16 A in case of Energy Dispersive X-ray Spectroscopy (EDX) probing (which was used for semi-quantitative elemental analyses for C, O, Ti, Al, S, and qualification as the average of three different points). The analytical accuracy of the performed EDX probing is ±2 %.

The thermal stability of the synthesized materials was evaluated with a Mettler Toledo TGA/DSC 3+ STARe system. The measurements were conducted from 25 °C to 850 °C at a heating rate of 10 °C per minute, under a nitrogen flow of 100 mL per minute.

The total acidity of the carbon catalysts was assessed using the Boehm titration method, following the standard protocol described in the literature [34,35]. A detailed description of the experimental procedure, including reagent concentrations, sample preparation, and titration conditions, is provided in our recent publication [32].

Solid-state ^{31}P MAS NMR spectra were recorded at room temperature using a 400 MHz Varian VNMRS spectrometer equipped with a 4 mm Varian/Chemagnetics T3 probe. The instrument operated at 9.4 T (161.9 MHz for ^{31}P) with a spinning frequency of 6 and 8 kHz. Samples were packed in 4 mm bio-solids cavern rotors provided by Phoenix NMR and sealed with non-vented PCTFE top spacers featuring two O-rings. The reported analysis is qualitative, and the experimental parameters included a $\pi/2$ pulse duration of 3.4 μs, a relaxation delay of 6 s, an acquisition time of 20 ms, and a total of 10000 scans. Chemical shifts were externally referenced to ammonium dihydrogen phosphate ($(NH_4)H_2PO_4$) with ^{31}P at 0.81 ppm [36]. A portion of the sample underwent a two-step dehydration process (details provided below). The 4 mm rotor was packed with a solid sample under an inert argon atmosphere inside a glovebox. Subsequently, 2 μL of liquid-phase trimethylphosphine (TMP) was added directly to the sample within the rotor. Excess TMP was removed by applying a vacuum of 10^{-6} mbar for 1.5 h at 100 °C using a custom-built setup, as described in the literature [37].

2.3.1. Dehydration process

Carbon-based materials such as the ones presented in this work exhibit high conductivity, complicating the tuning and matching of the probe. To address this problem, all the samples were diluted with pristine silica in a 2:1 silica-to-material ratio. A reference sample only constituted by silica was analyzed and didn't display any acidity, thus confirming that all the detected signals in the ^{31}P ss NMR spectra can be assigned to the carbon-based materials. Given the affinity of both pristine silica and the materials treated in this work with water, two different dehydration treatments were performed. Pristine silica was first calcined at 550 °C for 8 h, then treated for 2 h under vacuum (10^{-3} mbar) at room temperature. After this initial treatment, a physical mixture of silica and the material of interest was prepared inside a glovebox. Finally, the mixture was packed in the rotor. The packed rotor then underwent a second dehydration treatment at 100 °C overnight within the probe molecule system (custom-made setup) [38]. After this final stage, the rotor was transferred back into the glovebox, where the appropriate quantity of TMP was added before analysis.

The total acidity of the inorganic oxides was determined using temperature-programmed desorption with ammonia as a probe molecule in a Hiden Catlab gas analyzer coupled with a QGA Hiden quadrupole mass spectrometer. Prior to analysis, the catalyst sample (20–30 mg) was degassed at 150 °C for 1 h under Ar at a flow rate of 30 mL/min, followed by NH_3 adsorption at 60 °C for an hour under the gas mixture Argon and 5 % NH_3-He at a flow rate of 15 mL/min each. Next, NH_3 desorption was recorded under an Ar flow of 30 mL/min from 60 °C to 550 °C at a heating rate of 10 °C/min. The total acidity was calculated based on the integral area of the respective peaks obtained from the molecules desorbed per second versus the desorption temperature curve.

X-ray powder diffraction patterns were acquired in transmission mode on a MAR345 image plate diffractometer equipped with an Incoatec microfocus Mo anode (0.71073 Å, 1000 μA, 50 kV). Samples were prepared in glass capillaries (0.7 mm diameter, Hilgenberg GmbH), which were rotated 300° during the analysis for improved powder averaging and exposed for a total of 5 min. The raw diffraction images were integrated using the Fit2D software [39], using a NIST lanthanum hexaboride calibration standard for the determination of experimental setup parameters.

2.4. Cellulose pretreatment

The pretreatment of cellulose, such as ball milling, is a critical step to enhance its reactivity in subsequent processes by disrupting its crystallinity. This results in easier dissolution of cellulose fragments in the

reaction medium. Hence, ball milling was performed using a Fritsch Pulverisette 7 premium line apparatus. The experiments were performed in 45 mL stainless-steel (SS) milling bowls (Fritsch™ 50.9750.00) using 10 mm SS balls (Fritsch™ 55.0100.09). The treatment was done in two steps by following the previous work reported by our group [40]. First, 10 g of cellulose fibers (medium size) (Sigma Aldrich) was milled using five SS balls. The ball milling was conducted at room temperature (20 °C), and while the local heating was not monitored in situ, pauses were introduced to prevent potential overheating. Each cycle consisted of 15 min of milling at 300 rpm followed by a 5-min pause, with a total of 96 cycles, resulting in 24 h of ball milling.

In the second step, the ball milling was performed for a physical mixture of catalyst and ball-milled cellulose under different conditions due to the different quantities. In this case, 1 g of ball-milled cellulose and the required amount of catalyst (0.25 g in case of TiO_2 alone, and a total of 0.75 g of SO_3H/SX+ and TiO_2 (in case of a mix of both solids)) were combined with three SS balls. This treatment was carried out for 8 cycles of 15 min each at 300 rpm, with 5-min breaks, totalling 2 h of milling.

2.5. Catalytic activity

The catalytic activity of SO_3H/SX+ alone or in combination with Lewis acids was evaluated in a high-pressure autoclave stainless steel reactor (250 mL) (Parr Reactor, USA) in a 120 mL of milliQ water or biphasic medium i.e., MQ/THF, starting from cellobiose (≥99 %, Sigma Aldrich) as model soluble compound or cellulose fibers. The reaction was performed under a 4.8 bar N_2 atmosphere and 1700 rpm mechanical stirring. After the reaction, the catalyst was removed from the reaction mixture by filtration, and the filtrate was analyzed by high-pressure liquid chromatography (HPLC) equipped with an Aminex HPX87-H+ column (Bio-Rad, USA) with refractive index detector (RID) and diode array detector (DAD) using 5 mM H_2SO_4 as eluent at a flow rate of 0.55 mL/min. The column and detector temperatures were maintained at 65 °C and 50 °C, respectively. The total run time was 45 min. In the first part of our study, utilizing $AlCl_3$ as a homogeneous Lewis acid catalyst, we employed an HPLC system from WATERS, USA, equipped with an RID (2414, WATERS, USA). In the second part of the study, using heterogeneous Lewis acid catalysts, an HPLC system from the Agilent 1200 series (Germany) was used, featuring a DAD (G1315D, Agilent, Germany) coupled with a RID (G1362A, Agilent, Germany) in series due to the instrument availability. In both HPLC systems, the same column (Aminex 87H+) was used. The HPLC data in this study includes a ±5 % error margin, and the conversion and yield of all the known products were calculated based on the standard calibration curves of known concentrations of all compounds using the following formulae:

$$Cellobiose\ conversion = \frac{Moles\ of\ reacted\ cellobiose}{Moles\ of\ initial\ cellobiose} \times 100$$

$$Product\ yield = \frac{Moles\ of\ product\ obtained}{2 \times Moles\ of\ initial\ cellobiose} \times 100$$

In case of cellulose substrate, the following formulas were used to calculate the conversion and yield of the obtained products:

$$Cellulose\ conversion\ (wt.\%) = \frac{Mass\ of\ initial\ cellulose\ (g) - recovered\ mass\ cellulose\ (g)}{Mass\ of\ initial\ cellulose\ (g)} \times 100$$

Cellulose recovered mass = Total recovered weight of solid after filtration – weight of catalyst used in the reaction

Table 1
Physicochemical properties of the activated carbon catalysts.

Catalyst	XPS		N_2-physisorption			Boehm Titration
	S/C (% At. ratio)	N/C (%At. ratio)	BET surface area (m^2/g)	Pore Size (Å)	Pore Volume (cm^3/g)	Total Acidity (mmol/g cat.)
SX+	n.d.	n.d.	912	35	0.34	0.04
SO_3H/SX+	0.05	0.02	123	51	0.17	1.33
Compositional analysis on SO_3H/SX+						
Technique		%C	%S	%H	%N	%O
*XPS (wt.%)		79.9	3.34	n.d.	1.56	15.2
EDX (avg wt.%)		73.3	2.86	n.d.	n.d.	n.d.
CHNS (wt.%) [32]		71.9	3.22	2.13	0.8	n.d.

n.d. non-determined, *XPS wt.% values were calculated from the at.% obtained in XPS analysis.

$$Product\ yield\ (mol\%) = \frac{Moles\ obtained\ of\ the\ product}{Initial\ moles\ fed\ per\ unit\ of\ glucose\ in\ the\ cellulose} \times 100$$

* Molar mass of cellulose = 162.14 g/mol per unit of glucose.

2.6. Recycling runs

Recycling studies of the catalysts were conducted under optimized reaction conditions: cellobiose (1 g), SO_3H/SX+: TiO_2 (1/2 wt%), 150 °C, 4 h, MQ/THF, in a Parr reactor at 1700 rpm under 4.7 bar of N_2. After each reaction, the catalyst was filtered and washed with MQ water until the filtrate became clear, followed by drying overnight at 100 °C. The dried catalyst was then reused in the subsequent cycle. Multiple tests during the initial run were performed to collect sufficient used catalyst for the following cycles to ensure a consistent amount of catalyst throughout all the runs.

3. Results and discussion

3.1. Physicochemical properties of synthesized sulfonated carbon catalyst

Table 1 presents the physicochemical properties of the starting SX+ carbon and the synthesized SO_3H/SX+ catalyst. XPS results confirmed the successful grafting of sulfonic acid groups onto the surface of SX+, as indicated by the sulfur S_{2p} peak at the binding energy of 168.2 eV after functionalization [32], shown in Fig. S1. The surface S/C and N/C atomic ratios were determined and are reported in Table 1. The surface S/C (0.05) ratio is in line with our previous results [31].

The textural properties of activated carbon were assessed both before and after the functionalization with sulfonic groups (Table 1). The isotherms shown in Fig. 2(a) exhibit a Type I isotherm with an H4 hysteresis loop, indicating a combined microporous and mesoporous nature of both SX+ and SO_3H/SX+. The steep increase at low partial pressures is indicative of the presence of large amounts of micropores in the starting SX+ sample. The mesoporosity remains present even after sulfonic group functionalization. However, the surface area was notably reduced to approximately 123 m^2/g after the introduction of the SO_3H

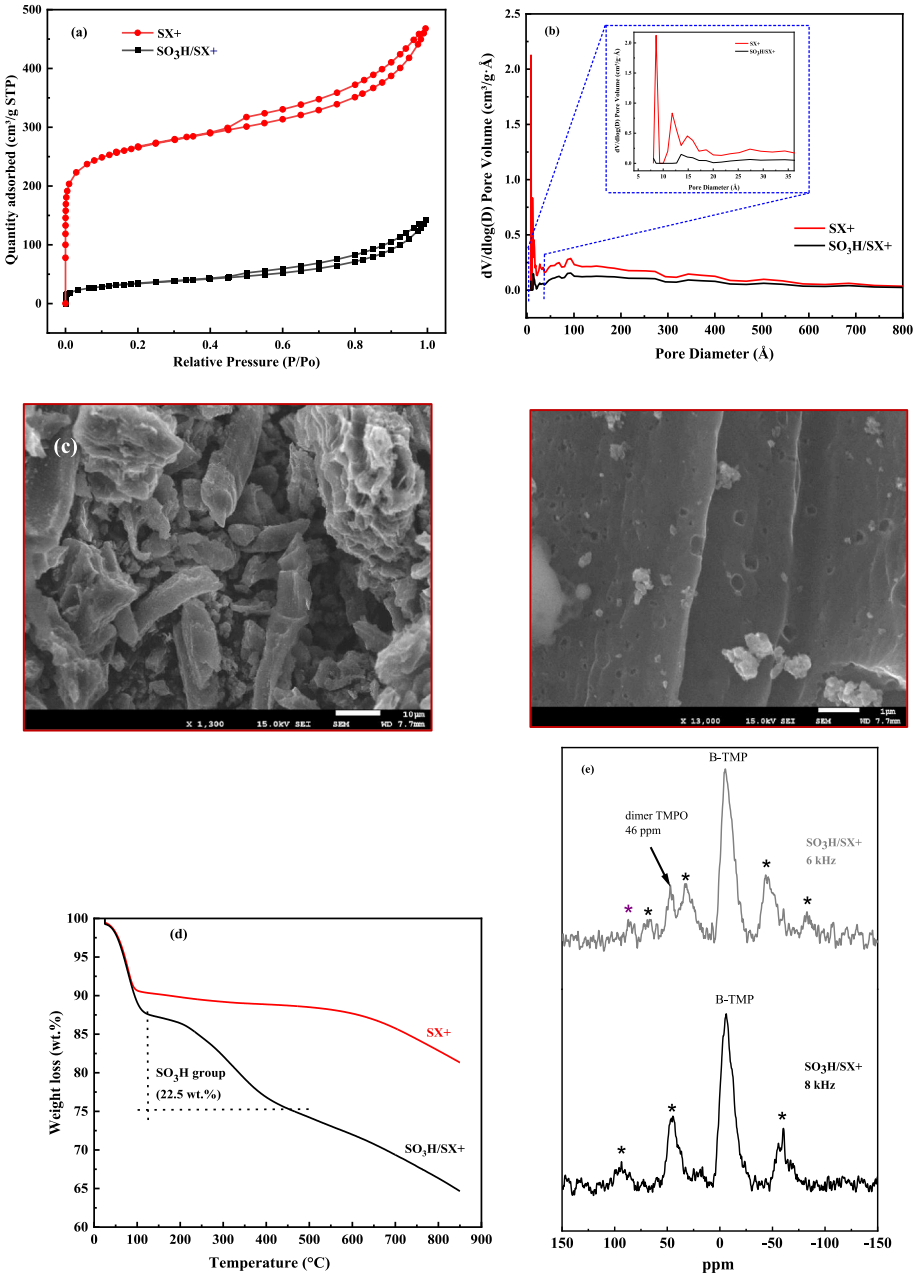

Fig. 2. (a) N_2 adsorption-desorption curves, (b) pore size distributions plots, (c) SEM images of SO_3H/SX+ (d) TGA curves of SX+ and SO_3H/SX+ materials, (e) ^{31}P ssNMR-TMP spectra of the SO_3H/SX + carried out at different spinning frequencies: 6 kHz (grey curve) and 8 kHz (black curve). Asterisks indicate the spinning sidebands.

groups. This reduction in surface area was likely due to micropores being blocked by the functional groups and/or small pores collapsing due to the conditions of organic chemistry functionalization. Indeed, the functionalized sample did not show the typical N_2 sorption feature of microporous solids anymore. This effect is also evident in the pore size distribution shown in Fig. 2(b), where there is a shift towards larger pore size after sulfonic group functionalization.

Fig. 2(c) presents the morphology of SO_3H/SX+, which highlights the structural characteristics of the grafted activated carbon. The synthesized catalyst (SO_3H/SX+) particles show a highly irregular and fragmented morphology, with randomly shaped structures. This is typical of the starting SX+ activated carbon (Fig. S2). No significant change in morphology was observed after sulfonic group grafting onto SX+. The elemental composition based on weight percentage (wt.%) was also determined using EDX, and the S amount is consistent with the wt.% values obtained from CHNS [32] and XPS analysis. The obtained data are presented in Table 1.

The thermal stability of SX+ and SO_3H/SX+ was evaluated by thermogravimetric analysis (Fig. 2(d)). The results obtained indicate that the sulfonic groups are stable up to 150 °C. Above this temperature, a notable weight loss of approximately 22 % was observed, which is attributed to the decomposition of the sulfonic groups, by comparison with the TGA curve of bare SX+ carbon, as shown in Fig. 2(d).

The total acidity of both solids, SX+ and SO_3H/SX+, was estimated using the Boehm titration technique and the obtained values are reported in Table 1. It was observed that the total acidity significantly increased to 1.33 mmol/g cat. after sulfonic groups grafting on activated carbon in comparison to pure SX+ (0.04 mmol/g cat.). This represents a 33-fold increase in total acidity following sulfonic group functionalization. This increased acidity of SO_3H/SX+ is essential for the conversion

of cellulose/cellobiose to 5-HMF, as the high acidity provides the necessary active sites for facilitating the dehydration and transformation reactions required for this selective process.

To gain deeper insights into the acidic properties of the two solids and identify potential differences stemming from their unique surface chemistry, ssNMR measurements were performed. It is widely recognized that probe molecules such as trimethylphosphine (TMP), trimethylphosphine oxide (TMPO), pyridine (Py), acetonitrile, and others, when analyzed via ssNMR, can provide key information about the nature of acid sites (Brönsted or Lewis) and their relative strength [36]. In this study, ^{31}P ssNMR with TMP as a probe molecule was employed to investigate the acidity of the materials. TMP was chosen due to its wide chemical shift range, which enables clear discrimination between Brönsted and Lewis acid contributions, as well as between Lewis acid sites of different strength. Additionally, the ^{31}P nucleus has 100 % natural abundance, avoiding the need for isotopic enrichment. It is important to note that the material must be thoroughly dehydrated before starting the analysis. In this context, considering the high conductivity of those materials, a dilution with a non-acidic solid was necessary to tune and match the Larmor frequency of the selected nucleus. Moreover, a reference sample only constituted by silica was analyzed and didn't display any acidity, thus confirming that all the detected signals in the ^{31}P ss NMR spectra can be assigned to the carbon-based materials (see Fig. S3). In this case, the carbon-based material was diluted with pristine silica (see Experimental Section), which is non-acidic (refer to Fig. S3). Interactions between TMP and Brönsted acid sites typically produce signals in the −2 to −5 ppm range, while interactions with Lewis acid sites result in resonances between −20 and −60 ppm [41]. However, TMP is highly susceptible to oxidation, even in the presence of trace amounts of oxygen, which can convert it into TMPO. This underscores the importance of maintaining strict control over experimental conditions [36].

Fig. 2 (e) displays the spectrum of the SO_3H/SX+ sample acquired at two different spinning frequencies, 6 kHz (grey line) and 8 kHz (black line), to identify the presence of spinning sidebands. A comparison of the two spectra reveals two main signals along with their respective sidebands. On the one hand, the signal centered at c. a. −4 ppm, corresponds to TMP bonded to Brönsted active sites [42]. On the other hand, the second signal centered at 46 ppm (visible only on the spectrum acquired at 6 kHz) is probably due to TMPO dimers formed after partial oxidation of physiosorbed TMP [42,43]. The high Brönsted acidity, combined with the low stability of TMP in the presence of oxygen, likely leads to the formation of TMPO dimers [43]. In summary, this analysis confirms that the SO_3H/SX+ material exhibits mainly Brönsted acidity.

The detailed characterization results for the synthesized heterogeneous Lewis acidic catalysts (γ-Al_2O_3, AlOOH, TiO_2) are shown in the supplementary file (Part 2: Heterogeneous Lewis acid catalysts characterization results).

3.2. Catalytic activity

3.2.1. Optimization of reaction conditions using SO_3H/SX+ catalyst and homogeneous Lewis acidic $AlCl_3$ catalyst

The cellobiose dehydration to 5-HMF reaction was studied first with different catalytic systems: blank run with no catalyst, unmodified SX+ carbon, SO_3H/SX+, $AlCl_3$, and $AlCl_3$ together with SO_3H/SX+, as shown in Fig. S9. The catalytic activity was evaluated in pure MQ water under reaction conditions, as previously reported by us [31], i.e. 1 g cellobiose, 0.3 g catalyst, 130 °C for 2 h under N_2 atmosphere. At the end of the reaction, the major products, namely glucose (GLU), fructose (FRU) and 5-HMF, were observed and quantified by HPLC. The blank run showed a negligible amount of conversion and traces of glucose formation, as expected under these reaction conditions. An 8.6 % cellobiose conversion with 4.2 % glucose yield was observed in the presence of pure SX+ carbon, because it already contains some B sites (due to surface O functional groups such as carboxylic acids) [44]. With SO_3H/SX+ catalyst, the cellobiose conversion increased to ~14 % with ~12 % yield of glucose due to the presence of sulfonic groups. This was anticipated, as cellobiose hydrolysis to glucose is driven by B acidity (Fig. 1), and especially strong acid sites as provided by the sulfonic groups, confirmed by ^{31}P ssNMR. The $AlCl_3$ soluble reagent ($AlCl_3.9H_2O$, 99 %, Alfa Aesar) was then used as a source of strong L acidity, which indeed gave a drastic increase in conversion (~60 %) and glucose yield (~30 %) using the same amount of $AlCl_3$ (0.3 g). In this case, fructose and a small amount of 5-HMF (1.7 %) were also observed. Similar observations were also made in the presence of a mixture of $AlCl_3$ and SO_3H/SX+ catalysts in a weight ratio of 1:1. These results conveyed a clear indication of the reaction being forwarded in the right direction, when detecting the formation of 5-HMF in the presence of $AlCl_3$.

Because isomerization of glucose to fructose is driven by L acidity, followed by 5-HMF formation catalyzed by the B acidity (Fig. 1), the next step was to optimize the ratio between B (SO_3H) and L ($AlCl_3$) acid sites, to obtain the best possible yield of 5-HMF. As shown in Fig. 3, the B/L ratio was optimized when running catalytic tests at 140 °C for 4 h of reaction with 0.5 g of catalyst, where ~80 % cellobiose was selectively converted into glucose with a ~77 % yield in pure MQ water reaction medium, using SO_3H/SX+ catalyst. The production of fructose and 5-HMF was not observed in the presence of pure SO_3H/SX+, due to the lack of Lewis acidic sites in this catalyst. When testing the dual catalytic system, i.e. SO_3H/SX+ solid in presence of soluble $AlCl_3$, the molar amount between the two components was varied with respect to the total acidity of sulfonic groups on the activated carbon by varying the SO_3H/Al ratio from 1:1 to 1:15, targeting 5-HMF as a final product (Fig. 3). The cellobiose conversion was increased from ~80 % to ~98 % after the addition of $AlCl_3$ to the reaction mixture. This also resulted in a higher glucose yield of ~87 % by varying the SO_3H/Al mol ratio to 1:4. At this SO_3H/Al mol ratio (1:4), traces of 5-HMF started to be observed and increased together with an increasing yield of fructose and decreasing yield of glucose, along the increase of SO_3H/Al mol ratio till 1:15. However, at this highest ratio (1:15), the glucose yield drastically decreased to ~23 % without significantly increasing the yield of fructose and 5-HMF, demonstrating the reaction acceleration in a non-selective manner at higher concentration of $AlCl_3$. Nevertheless, these results indicate that on increasing the amounts of Al^{3+}, the reaction proceeds in the forward direction and the formation of fructose and 5-HMF is started.

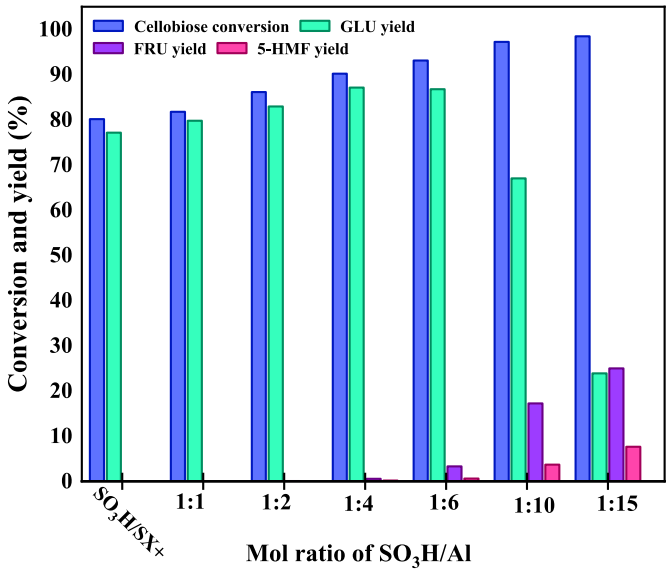

Fig. 3. Effect of Brönsted and Lewis acid ratio when using SO_3H/SX+ and soluble $AlCl_3$ as a catalytic system (reaction conditions: 140 °C, 4 h, 1 g cellobiose, SO_3H/SX+ = 0.5 g, 120 ml MQ, 1700 rpm, 4.7 bar N_2).

In the next step, the catalytic activity of SO_3H/SX+ (Brönsted acid) combined with $AlCl_3$ (Lewis acid) was evaluated in three different solvent media, i.e., MQ, MQ/THF (1:3 vol%), and MQ-NaCl/THF (1:3 vol %) to understand the effect of the reaction medium. NaCl was added to the MQ water until it reached saturation. In the literature, biphasic systems have shown the potential for achieving high HMF yields from cellulose/glucose by continuously extracting HMF from the aqueous phase to the organic one, which helps to reduce its conversion into undesirable byproducts such as LA, FA, and humin [26,45]. Extractive solvents such as THF, MIBK, and DMSO are mostly used, with THF being particularly attractive due to its lower boiling point, facilitating easy reusability and final separation of 5-HMF. Moreover, the addition of NaCl in the biphasic medium enhances the yield of 5-HMF by shifting the equilibrium towards 5-HMF by increasing the partition coefficient, so bringing even more 5-HMF into the organic phase [46]. The reaction was performed with a low SO_3H/Al ratio (1:4), where only trace amounts of 5-HMF were obtained in pure water (Fig. S3). The results, presented in Fig. 4, indicate that different reaction media produced distinct product distributions. As described above, pure MQ water permitted cellobiose hydrolysis to glucose, resulting in a remarkably high glucose yield (~87 %) with ~90 % conversion of cellobiose. The monophasic MQ/THF system drove the reaction further, yielding a different product distribution: glucose (~53 %), fructose (~28 %), and 5-HMF (~10 %), with almost complete conversion of cellobiose under the same reaction conditions. This might be attributed to favorable properties such as enhanced mixing, mass transfer, and reaction kinetics in MQ/THF reaction media. However, in the biphasic MQ-NaCl/THF medium, the conversion and resulting product yields were unexpectedly lowered due to the complexity of phase behaviors. These results demonstrate that the reaction product distribution is highly influenced by the reaction medium. The product distribution from cellobiose hydrolysis is affected not only by the selected solid acid catalyst but also by the synergistic effects of the solvent. Consequently, MQ/THF was considered the optimum solvent for further optimizations, based on these results.

3.2.2. *Effect of reaction temperature*

The effect of temperature on cellobiose hydrolysis to 5-HMF was studied by varying the reaction temperature from 120 to 150 °C with intervals of 10 °C at the previously optimized reaction conditions (Fig. 5). At each temperature, the reaction was performed in presence of various catalysts such as SO_3H/SX+, $AlCl_3$, and SO_3H/SX+ with $AlCl_3$.

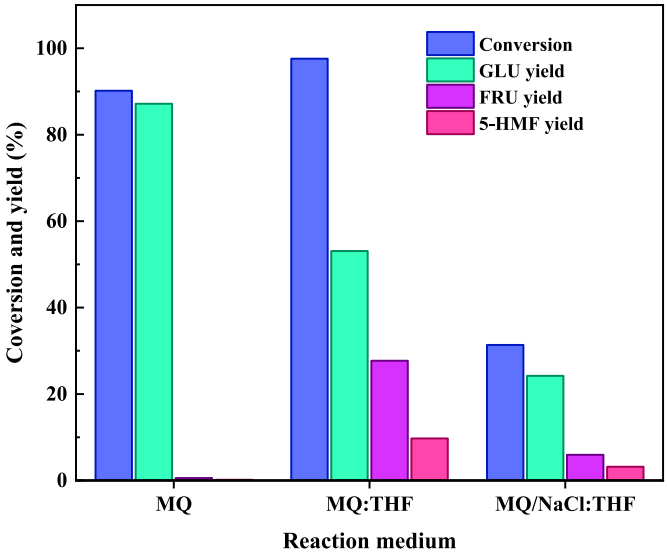

Fig. 4. Effect of reaction solvent (reaction conditions: 140 °C, 4 h, 1 g cellobiose, SO_3H/SX+ = 0.5 g, SO_3H/Al = 1:4, 1700 rpm, 4.7 bar N_2).

The blank run was performed only in the extreme points of our reaction conditions, i.e., 120 °C and 150 °C. The amounts of SO_3H/SX+ and $AlCl_3$ were taken to reach a SO_3H/Al ratio of 1:4 in the case of mixtures. As shown in Fig. 5 (a), the cellobiose conversion was found to increase with the reaction temperature. At the lowest temperature (120 °C), the blank run shows no conversion, while in the presence of a catalyst, i.e., SO_3H/SX+, $AlCl_3$, or both together, a conversion of 50–70 % was reached. This was found to increase to ~99 % with the temperature. A higher yield of glucose (~18–81 %) (Fig. 5(b)) was formed at the lower temperatures until 130 °C, whereafter it was observed to decline to approximately 33 % with an increasing yield of fructose (~33 %) (Fig. 5 (c)) and 5-HMF (~20 %) (Fig. 5(d)) at 150 °C in the presence of the $AlCl_3$ or SO_3H/SX+: $AlCl_3$ (1:4) catalysts. The comparison between the catalytic activity can be seen clearly with respect to 5-HMF formation at different temperatures. At low temperature (<130 °C), the reaction did not proceed further in the direction of 5-HMF formation (Fig. 5(d)), whereas higher temperature (>140 °C) enhanced the dehydration step, resulting in a higher yield of 5-HMF. This is due to the endothermic nature of fructose dehydration [47–49], as 5-HMF is expected to be obtained via fructose dehydration. However, even at the highest temperature (150 °C), SO_3H/SX+ alone showed a very low yield in 5-HMF (~8 %) due to the absence of Lewis acidic sites in this catalyst. When using pure $AlCl_3$ or a mix together with SO_3H/SX+, a higher 5-HMF yield (20–23 %) was obtained with small amounts of rehydration products i.e., LA (~2 %) and FA (~7 %) (not shown on plots due to their trace amounts) due to the strong acidity of homogeneous $AlCl_3$. The pH of the reaction mixture was measured after the addition of $AlCl_3$ in the solution and was found to be in the range of pH = 3–4. In previous articles [45,50,51], it has been reported that Al^{3+} cations act differently in different pH regimes in aqueous medium. Some species can be formed such as hexa-coordinated $[Al(aq)]^{3+}$ at pH < 3.0, and hexa-coordinated hydroxo monomers ($[Al(OH)(aq)]^{2+}$), ($[Al(OH)_2(aq)]^{+}$), dimers ($[Al_2(OH)_2(aq)]^{4+}$) or trimers ($[Al_3(OH)_4(aq)]^{5+}$), at pH values of 3.0–7.0, some presenting Brönsted acidity. $AlCl_3$ dominates the reaction kinetics due to its homogeneous nature in aqueous medium, which provides a strong L and B acidity. Therefore, the maximum 5-HMF yield did not change much in the presence of SO_3H/SX+: $AlCl_3$ compared to $AlCl_3$ alone. However, different product distributions have been observed in presence of each of the three catalytic systems, i.e. pure SO_3H/SX + displayed ~32 % of glucose with ~34 % of fructose and lower 5-HMF yield (7.7 %) with no rehydration products, while $AlCl_3$ alone gave 4 % of glucose, 21 % of fructose with 23 % of 5-HMF together with LA and FA at 150 °C. Both catalysts together (SO_3H/SX+ and $AlCl_3$) gave ~33 % glucose, ~27 % fructose and ~21 % of 5-HMF, also with LA and FA. These results possibly demonstrate that product distribution is highly influenced by the reaction kinetics in the presence of various catalytic systems at the highest temperature. Hence, 150 °C was considered as an optimum temperature with respect to the 5-HMF yield for further studies.

Finally, the cellobiose hydrolysis reaction was evaluated at higher SO_3H/SX+: Al ratio (1:10), where an enhanced 5-HMF yield (3.5 %) was obtained at lower temperature (140 °C) in pure MQ (Fig. 3). The reaction was also studied in the presence of the commercial Amberlyst-15 reference acid catalyst at the optimized reaction conditions. The results obtained are presented in Fig. 6. A significant increase in 5-HMF yield from approximately 21 %–~51 % was observed with the SO_3H/Al ratio 1:10 at 150 °C after 4 h in MQ/THF medium. While in the presence of Amberlyst-15 catalyst, a strong acidic catalyst, 97 % of cellobiose conversion and 76 % of glucose, with only ~9 % of 5-HMF yield, were found under similar reaction conditions. Hence, here it is concluded that a strong acid catalyst containing both Brönsted and Lewis acidity and higher reaction temperature (≥140 °C) is required to obtain a high yield of 5-HMF from cellobiose. However, despite achieving a high 5-HMF yield in the presence of the $AlCl_3$ catalytic system, several drawbacks, correlated to the use of a homogeneous catalyst, such as equipment corrosion and challenging catalyst

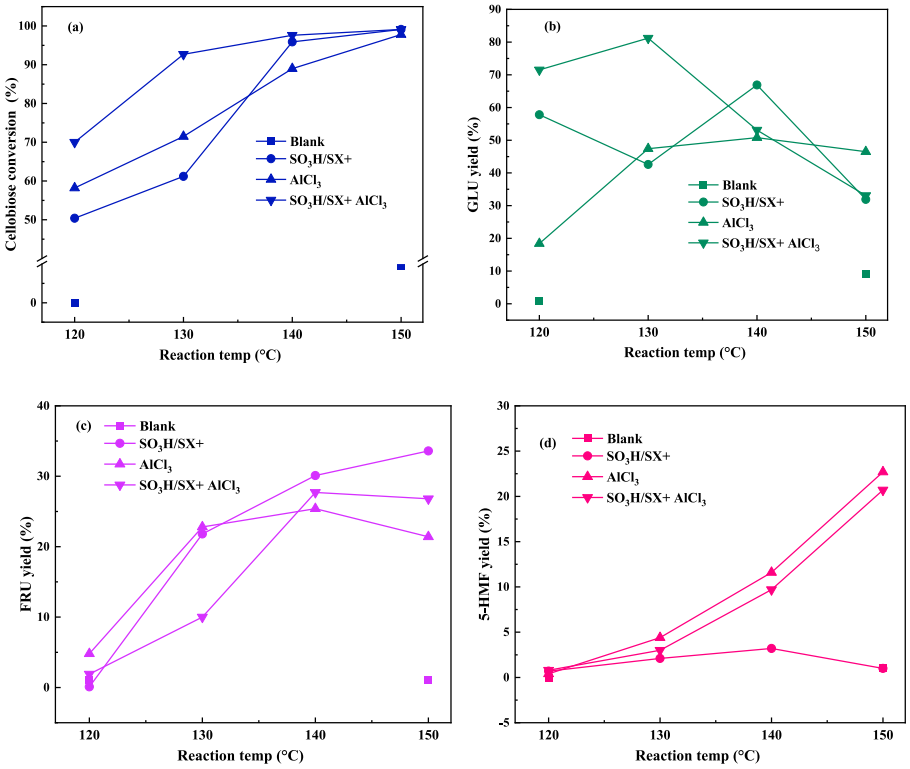

Fig. 5. Effect of reaction temperature on cellobiose hydrolysis reaction in the presence of various catalysts (a) Cellobiose conversion, (b) Glucose yield, (c) Fructose yield, (d) 5-HMF yield (reaction conditions: 4 h, 1 g cellobiose, $SO_3H/SX+$ = 0.5 g, SO_3H/Al = 1:4, MQ/THF (1/3 vol%), 1700 rpm, 4.7 bar N_2).

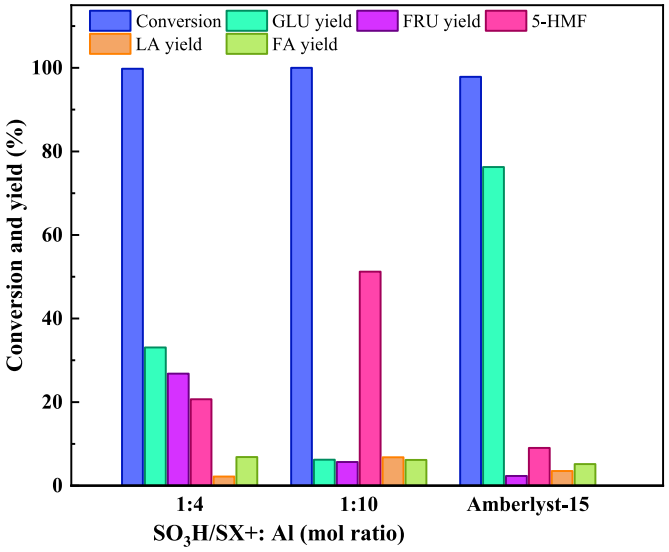

Fig. 6. Comparison of SO_3H/SX + $AlCl_3$ catalyst with highly acidic Amberlyst-15 catalyst (reaction conditions: 150 °C, 4 h, 1 g cellobiose, $SO_3H/SX+$ = 0.5 g, Solvent: MQ/THF (1/3 vol%), 1700 rpm, 4.7 bar N_2).

recycling, are associated with it. Therefore, in the next section of this study, we have replaced the homogeneous Lewis acid ($AlCl_3$) by heterogeneous Lewis acidic catalysts such as γ-Al_2O_3, AlOOH and TiO_2.

3.2.3. *Transitioning from homogeneous Lewis acid ($AlCl_3$) to heterogeneous Lewis acid catalysts*

In this section, we have studied three heterogeneous Lewis acidic catalysts, namely γ-Al_2O_3, AlOOH and TiO_2 in combination with our synthesized sulfonated activated carbon ($SO_3H/SX+$) for cellobiose hydrolysis to 5-HMF, in a high-pressure Parr reactor at the optimized reaction conditions, as described in the above section. These heterogeneous Lewis acidic catalysts were synthesized and characterized by N_2-physisorption, XRD, NH_3-TPD, TGA and SEM and all the characterization data are presented in the supplementary file (Part 2: Heterogeneous Lewis acid catalysts characterization results). The ratio between the heterogeneous Lewis acidic catalyst and $SO_3H/SX+$ was optimized, starting with an initial molar ratio ($SO_3H/SX+$: Al) of 1:10, as previously optimized in the earlier section using $AlCl_3$, a homogeneous Lewis acidic catalyst.

First, the catalytic activity of γ-Al_2O_3 was tested for cellobiose hydrolysis under the optimized conditions (150 °C, 4 h, MQ/THF) by varying the $SO_3H/SX+$: Al ratio between 1:10, 1:50, and 1:100 and the obtained results are shown in Fig. S10. A 98 % cellobiose conversion with high yield of glucose (56 %), ~14 % of fructose and a low (8 %) 5-HMF yield were observed at $SO_3H/SX+$: Al mol ratio of 1:10. No notable change in conversion and products yield were observed on further increasing the ratio between $SO_3H/SX+$: Al (1:50 and 1:100), due to the insignificant acidic sites and total acidity (0.17×10^{-2} mol/g cat.) of this Al-based material, as reported in Table S1 and Fig. S6(a), respectively.

Second, boehmite (AlOOH) combined with $SO_3H/SX+$ (mol ratio = 1:10) was tested under the same reaction conditions and yielded 8 % of 5-HMF with ~33 % of glucose, 18 % of fructose over 81 % cellobiose conversion (Fig. 7(a)). By contrast, a higher catalytic activity of TiO_2 combined with $SO_3H/SX+$ (wt. ratio = 1:1) catalyst was observed, which yielded 41 % of 5-HMF, 21 % of glucose and 2 % fructose with complete conversion of cellobiose at the same reaction conditions (Fig. 7 (a)). This superior catalytic activity of TiO_2 might be attributed to its higher total acidity (2.40×10^{-2} mol/g cat.) and the presence of strong acidic sites compared to that of boehmite (1.04×10^{-2} mol/g cat.) and γ-Al_2O_3 (0.174×10^{-2} mol/g cat.) (Table S1). This means that the TiO_2 combined with $SO_3H/SX+$ in a wt. ratio = 1:1 corresponds to 0.012 mol of TiO_2 (based on acid sites). As shown in the TPD curve (Fig. S6(c)),

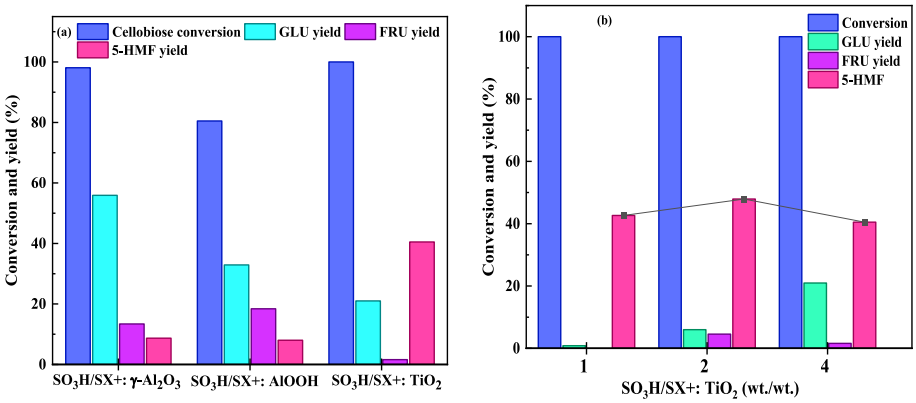

Fig. 7. (a) Influence of various heterogeneous Lewis acidic catalysts (γ-Al_2O_3, AlOOH and TiO_2) combined with SO_3H/SX+ [SO_3H/SX+: γ-Al_2O_3 ratio (1:10) in mols; SO_3H/SX+: AlOOH ratio (1:10) in mols; SO_3H/SX+: TiO_2 ratio (1:1 wt%)] (b) Effect of SO_3H/SX+: TiO_2 ratio on cellobiose conversion and 5-HMF yield (reaction conditions: 150 °C, 4 h, MQ:THF, 1 g cellobiose, SO_3H/SX+ = 0.5 g, 1700 rpm, 4.7 bar N_2).

TiO_2 exhibits both weak (desorption peak at ~156 °C) and strong acidic sites (desorption peak at 325 °C), while AlOOH demonstrates only weak acidic sites (peak at 180.4 °C) (Fig. S6(b)). Both materials exhibit a mesoporous nature with similar specific surface area (~235–246 m^2/g) and pore sizes (1.9–3.4 nm) (Table S1, Fig. S4). These findings suggest that TiO_2 together with SO_3H/SX+ might be a competitive catalytic system among all these heterogeneous Lewis acidic catalysts tested, likely due to its higher acidity, primarily resulting from stronger acidic sites.

Then, the weight ratio between SO_3H/SX+ and TiO_2 catalysts was optimized to achieve the highest possible yield of 5-HMF. It varied between 1, 2 and 4 by varying the TiO_2 amount, namely taking 0.5 g, 0.25 g and 0.125 g in the presence of 0.5 g SO_3H/SX+, respectively. The results obtained are presented in Fig. 7(b). A complete conversion of cellobiose was achieved at all three ratios, while different product distributions of glucose, fructose and 5-HMF were observed. At the SO_3H/SX+: TiO_2 ratio of 1, a 40 % yield of 5-HMF with traces of glucose was observed, while by reducing the amount of TiO_2 (0.25 g) at the ratio 2, a ~48 % yield of 5-HMF with 6 % of glucose and 5 % of fructose was observed. That is similar to the yield obtained in the presence of SO_3H/SX+: Al at the ratio of 1:10 in the presence of homogeneous $AlCl_3$ catalyst under the same reaction conditions (Fig. 6). Furthermore, by further reducing the amount of TiO_2 to 0.125 g (to achieve a ratio of 4), a reduction in 5-HMF yield (41 %) was observed, along with a slightly higher glucose yield (~21 %). These results demonstrate that different reaction kinetics were followed with varying amounts of TiO_2. A separate and detailed kinetic study would be required to explain this more clearly. However, the objective of this study was not to investigate the kinetics of the cellobiose reaction. Therefore, considering the highest yield of 5-HMF (~48 %), the SO_3H/SX+: TiO_2 ratio of 2 was considered optimal.

As heterogeneous catalyst recycling is crucial, recycling runs were performed under optimized conditions (Fig. S11). The SO_3H/SX+: TiO_2 system could be recovered easily as a physically mixed powder and reused. It showed a gradual decrease in catalytic activity over multiple cycles of use. Specifically, a decline in cellobiose conversion (from 100 % to 82.8 %) and HMF yield (49 %–21 %) was observed over the recycling runs, together with an increase in glucose yield (6.8 %–18 %). This increase in glucose yield during the recycle runs suggests a reduced rate of glucose dehydration reaction, possibly due to TiO_2 Lewis acidity deactivation by humins deposition. Hence, TEM, EDX and Boehm titrations analyses were performed on the physical mixture of SO_3H/SX+ and TiO_2 catalysts before and after three catalytic cycles. The obtained EDX results confirmed the presence of S, C, O, and Ti in both fresh and used samples, indicating the structural integrity of the catalyst components. In the fresh sample, TiO_2 exhibited a spherical particle-like morphology, which became larger and more agglomerated after the third use. Additionally, the amount of carbon present in the used mixture was higher than in the fresh mixture (see Fig. S12 (b) in supplementary information). This might be due to the deposition of humin on the active sites of TiO_2, which could lead to a reduction in the total acidity of the material. This observation is consistent with the Boehm titration results obtained for the physical mixture of catalysts. The fresh mixture showed an acidity of 1.26 mmol/g of catalyst, which decreased to 0.54 mmol/g in the recovered catalyst after 3 runs. This reduction may be attributed to the accumulation of humin on the surface of the active sites, which could also contribute to the formation of larger TiO_2 particles, as observed in Fig. S12 (b) (supplementary information). Indeed, a similar reduction in the catalytic activity during the recycle runs using TiO_2 catalyst was reported in our earlier work [7] and TiO_2 catalyst activity was restored by heating at 400 °C for 1 h to remove the brown deposited products, possibly humin, from the active sites. After this regeneration treatment, TiO_2 regained its catalytic activity at a level comparable to that of the fresh catalyst. Although such reactivation procedures could potentially address the present limited deactivation issue, they were not explored in the current study. This is because the catalyst is a physical mixture of SO_3H/SX+ and TiO_2 catalyst, and heating above 200 °C could lead to the degradation of sulfonic acid groups from the activated carbon surface. Hence, in our current study, the catalyst was barely washed and dried between the consecutive runs, and it is remarkable that it was still active and capable of giving HMF. Regeneration methods such as heating under an inert atmosphere or acid washing could be explored but would require some optimization. However, this lies beyond the scope of the present study and can be considered in future work on catalyst deactivation, together with more advanced characterizations able to tackle physical mixtures in a meaningful way.

3.3. Cellulose direct transformation to 5-HMF

Cellulose hydrolysis is challenging due to its microcrystalline structure, reinforced by intra-, intermolecular, and inter-sheet hydrogen bonds, making it insoluble in most solvents such as water. However, techniques like ionic liquids (though expensive and toxic), supercritical water, and ball milling have been used to reduce crystallinity and break cellulose into oligomers to enhance its reactivity [40]. In our study, we used ball milling to mechanically reduce cellulose crystallinity, facilitating its transformation. The conversion of cellulose to 5-HMF was studied in the presence of our best catalytic system, namely SO_3H/SX+: TiO_2, and TiO_2 alone for comparison, under optimal reaction conditions (150 °C, 4 h, MQ:THF, SO_3H/SX+: TiO_2 = 2) using ball-milled cellulose as a substrate (see section 2.4 cellulose pretreatment for more details). TiO_2 alone showed only ~4 % yield in 5-HMF with traces of cellobiose, glucose, and fructose, while TiO_2 with SO_3H/SX+ produced a higher

Table 2
Transformation of cellulose to 5-HMF.

Reaction conditions	Cat. amount	Feed	Cellulose conversion (wt.%)	Cellobiose (mol %)	Glucose (mol %)	Fructose (mol %)	5-HMF (mol%)
150 °C, 4 h	TiO_2 (0.25 g)	1 g ball milled cellulose combined with a catalyst	70	0.3	0.8	0.4	4
150 °C, 4 h	TiO_2 + SO_3HSX+ (0.25 + 0.50 g)		52	0.2	2.5	0.6	10
150 °C, 24 h			66	~0.1	~0.6	~0.3	24

yield of 5-HMF (10 %) and 3 % glucose after 4 h of reaction, due to the strong efficiency of sulfonic groups grafted on activated carbon in cleaving glycosidic bonds in cellulose. Additionally, extending the reaction time to 24 h led to a significant increase in 5-HMF yield, reaching ~24 % under the same reaction conditions using TiO_2 mixed with $SO_3H/SX+$ as catalyst (Table 2). These results further confirmed the synergy between $SO_3H/SX+$ and TiO_2 in promoting cellulose valorization. This synergy between $SO_3H/SX+$ and TiO_2 played a pivotal role in cellulose conversion, where $SO_3H/SX+$ permitted depolymerization by breaking the glycosidic bonds of cellulose and TiO_2 enhanced downstream glucose isomerization and dehydration. Together, they enabled a more efficient and selective pathway toward 5-HMF production. Further optimization of reaction parameters for the direct conversion of raw cellulose into 5-HMF may improve the selectivity and yield of the target molecule, 5-HMF, but this also goes beyond the scope of the present contribution.

3.4. Isolation of 5-HMF

The separation and isolation of 5-HMF from the reaction mixture is the real challenge for industrial viability of the process. Therefore, we have isolated and purified the HMF from the low-boiling-point reaction mixture, i.e., monophasic MQ/THF, by following the simple liquid-liquid extraction technique reported in our previous work [52]. As shown in the flow diagram (Fig. S13 (i)), the catalyst was separated from the reaction mixture by vacuum filtration, followed by the isolation and purification of 5-HMF. The phase separation of the reaction mixture was performed by adding NaCl in the monophasic MQ/THF reaction solvent until the NaCl saturated the solution to make the separation process easier [53,54]. During the addition of NaCl, separation of the two phases of the reaction mixture was visible as the NaCl reached close to the saturation level. The color of the aqueous layer was light yellowish, while the organic layer (THF) was more brownish due to the presence of 5-HMF. Further, the reaction mixture was transferred to a separating funnel and vigorously shaken to enhance the mass transfer between the layers. Then, it was left still for 2 h for the complete separation of the two layers. After the separation of the THF layer, the THF was evaporated at 30 °C for 30 min using a rotary evaporator (IKA, Germany). Thereafter, a viscous residue that contained 5-HMF was obtained. To enhance the purity of the obtained product (5-HMF), it was again dissolved in THF solvent (30 mL). The THF layer was again mixed with NaCl-saturated water by keeping the volume ratio constant to 1:3, as we have used in our reaction. Then further steps were again followed to separate the THF layer from the mixture. Finally, a small amount of this viscous residue was dissolved in pure MQ water and filtered through a 0.22 μm syringe filter and analyzed by HPLC. The pictures of the final products separated at different stages from the reaction mixture are shown in Fig. S13 (ii) in the supplementary information. The HPLC equipped with DAD (286.4 nm) and RI detector confirmed the presence of 5-HMF with ~98 % purity on the basis of area obtained with the detectors. The obtained chromatograms of extracted 5-HMF via RID and DAD are shown in the supplementary file Fig. S14(a) and S14(b), respectively. The purity of the peak of detected 5-HMF was confirmed by DAD detection at 286.4 nm (Fig. S14(c)), and the retention time of 5-HMF was confirmed by running the standard 5-HMF sample in HPLC using both detectors, as shown in Fig. S14(c) and S14(d). With that, the process was complete, and the usefulness of our catalytic system based on sulfonated carbon mixed with Lewis acid providers is demonstrated.

3.5. Comparison with literature

Table S4 (supplementary information) provides a comprehensive analysis of various catalytic systems and reaction conditions reported in the literature for the conversion of glucose and cellobiose into 5-HMF, alongside our obtained results using the $SO_3H/SX+$ and TiO_2 catalytic system. Both homogeneous catalysts, such as rare earth metal chlorides and $AlCl_3$, and heterogeneous catalysts, including ion-exchange resins and Fe_3O_4 nanoparticles, are reported in the literature, utilizing various reaction solvents like water, organic solvents (THF, DMSO), and ionic liquids ([BMIM]Cl, $[IMEP]BF_4$), which significantly influence reaction efficiency. The feedstocks used in these studies primarily include glucose and cellobiose, with the choice of feedstock also affecting reaction efficiency, catalyst performance, and overall yield. As shown in the table, for cellobiose, higher reaction temperatures and longer reaction times have been reported by H. Kimura (2013) [55], A. Bhalkikar (2015) [56], and Y. Song (2014) [57], compared to glucose, due to its more complex structure and need to break the glycosidic bonds. Our study follows similar reaction conditions to those used for glucose conversion but starts from cellobiose. Indeed, we utilize here a lower reaction temperature and shorter reaction time (150 °C, 4 h), comparable to the conditions reported by P. Wrigstedt (2016) [58], Parveen and Upadhyayula (2017) [59], W. Guo (2020) [60] using glucose as the feedstock. The highest 5-HMF yield (71 %) was achieved in a catalyst-free DMSO-water system at comparatively higher reaction temperature and prolonged time, while other catalytic systems resulted in moderate to high yields (48–66.4 %). In comparison, in our study, A ~50 % 5-HMF yield was achieved utilizing $SO_3H/SX+$: TiO_2 in MQ/THF at 150 °C for 4 h, which demonstrates its competitiveness with existing methodologies. The $SO_3H/SX+$: TiO_2 combination has shown better catalytic activity than other catalytic systems, such as Fe_3O_4 nanoparticles (23.4 % HMF yield) and ionic liquids ($[IMEP]BF_4$, 39.2 % HMF yield). The use of a heterogeneous catalyst offers notable advantages in recyclability and ease of separation compared to homogeneous catalysts like $AlCl_3$, which are often corrosive, costly and challenging to recover. Additionally, the selection of MQ/THF as a solvent provides an alternative to DMSO and ionic liquids, which, despite their efficacy, pose challenges in complex downstream processing. Overall, this study presents a balanced and efficient approach in terms of yield, catalyst reusability, and reaction conditions, altogether highlighting the potential of cellulose or cellobiose as a viable and sustainable feedstock for 5-HMF production.

4. Conclusion

The study successfully demonstrated the functionalization of activated carbon (SX+) with sulfonic acid groups (SO_3H) using the diazonium coupling method, significantly enhancing the B acidity of the activated carbon. The B acidity imparted by SO_3H groups, confirmed by XPS, ^{31}P ssNMR and Boehm titration, played a key role in driving the cellobiose hydrolysis reaction. The $SO_3H/SX+$ alone is very effective for cellobiose hydrolysis (~80 %) to glucose (~77 %) in pure water medium due to its higher Brönsted acidity provided by sulfonic groups. The $SO_3H/SX+$ catalyst, in combination with Lewis acids like homogeneous $AlCl_3$, exhibited promising catalytic activity for the conversion of cellobiose to 5-HMF. The ratio between SO_3H and Al, together with the

reaction solvent, played a key role in desired product formation. In addition, a higher reaction temperature (≥140 °C) was required to drive the reaction further towards 5-HMF formation. A maximum ~47 % yield of 5-HMF was obtained at optimized reaction conditions, i.e. 150 °C, 4 h, SO_3H/SX+: Al ratio 1:10, and MQ/THF reaction medium. However, $AlCl_3$ dominates the reaction due to its strong acidic and homogeneous nature. Consequently, efforts were made to transition from homogeneous $AlCl_3$ to heterogeneous Lewis acid catalysts, particularly TiO_2, which further improved the yield to ~50 % 5-HMF at SO_3H/SX+: TiO_2 weight ratio of 2:1. TiO_2 gave a higher yield of 5-HMF than AlOOH and γ-Al_2O_3 catalysts due to its higher total acidity (2.4×10^{-2} mol/g cat.) mainly due to presence of stronger acidic sites. Both the catalysts together SO_3H/SX+: TiO_2 (in wt. ratio = 2) provided a comparatively higher yield of 5-HMF (~24 % in 24 h of reaction) than TiO_2 alone for direct ball-milled cellulose conversion. This was attributed to the strong efficiency of SO_3H groups of sulfonated activated carbon catalyst to break the glycosidic bonds of cellulose. Finally, the successful isolation of high-purity 5-HMF (~98 %) derived from cellobiose underscores the potential of this catalytic system for sustainable biomass valorization. Moreover, this study enhances the understanding of the role of Brönsted and Lewis acid sites in the design of bifunctional acidic catalysts, such as I4@BATEOS/SO_3H, recently synthesized by A. Tonelli et al. [32] from our group.

CRediT authorship contribution statement

Richa Tomer: Writing – review & editing, Writing – original draft, Visualization, Validation, Methodology, Investigation, Formal analysis, Data curation, Conceptualization. **Alessia Tonelli:** Methodology, Data curation. **Anthony Morena:** Writing – review & editing, Writing – original draft, Methodology, Data curation. **Luca Fusaro:** Writing – review & editing, Methodology, Data curation. **Vera Meynen:** Writing – review & editing. **Carmela Aprile:** Writing – review & editing. **Sophie Hermans:** Writing – review & editing, Visualization, Validation, Supervision, Resources, Project administration, Funding acquisition, Conceptualization.

Conflicts of interest

There are no conflicts of interest to declare.

Acknowledgements

The authors appreciatively acknowledge IMCN, Université catholique de Louvain (UCLouvain), Belgium, for providing all the necessary facilities to conduct this research. Additionally, we extend our thanks to Jean-François Statsyns for his assistance in BET and TGA analysis, to Timothy Steenhaut for obtaining the X-ray diffraction patterns and to Fabien Drault for performing TEM-EDX analysis. We further extend our gratitude to MOCA-Mineral & Organic Chemical Analysis platform, UCLouvain, for providing the HPLC facility and University of Namur for providing the Solid-state ^{31}P ssNMR facility, in particular Mr. Oliver Garot for the support in set-up development. This project has received funding from the FWO and F.R.S.-FNRS (Belgium) under the Excellence of Science (EOS) program ("PHOSPORE" - EOS reference number: 40007504).

Appendix A. Supplementary data

Supplementary data to this article can be found online at https://doi.org/10.1016/j.biombioe.2025.108320.

Data availability

All data supporting this study have been included in the manuscript and supplementary information.

References

[1] Y. Lei, G. Zhu, X. Liu, X. Wu, B. Fu, Y. Chen, Comparative assessment of 5-hydroxymethylfurfural production: economic viability and environmental performance of five conceptual bioprocesses, Biomass Bioenergy 201 (2025) 108118, https://doi.org/10.1016/J.BIOMBIOE.2025.108118.
[2] A.R. Mankar, A. Pandey, A. Modak, K.K. Pant, Microwave mediated enhanced production of 5-hydroxymethylfurfural using choline chloride-based eutectic mixture as sustainable catalyst, Renew. Energy 177 (2021) 643–651, https://doi.org/10.1016/j.renene.2021.05.157.
[3] A. Mukherjee, M.J. Dumont, V. Raghavan, Review: sustainable production of hydroxymethylfurfural and levulinic acid: challenges and opportunities, Biomass Bioenergy 72 (2015) 143–183, https://doi.org/10.1016/J.BIOMBIOE.2014.11.007.
[4] X. Shi, X. Xing, W. Liu, M. Ruan, Y. Guan, G. Lyu, H. Gao, S. Xu, Cellulose conversion to 5-hydroxymethylfurfural via a simple and efficient phosphate-doped hafnium oxide catalyst, Renew. Energy 226 (2024) 120425, https://doi.org/10.1016/j.renene.2024.120425.
[5] J. Cai, C. Xu, W. Shi, S. Wu, Selective HMF synthesis from glucose via microwave-assisted metal chloride catalysis, Biomass Bioenergy 181 (2024) 107060, https://doi.org/10.1016/J.BIOMBIOE.2024.107060.
[6] K. Nakajima, R. Noma, M. Kitano, M. Hara, Selective glucose transformation by titania as a heterogeneous Lewis acid catalyst, J. Mol. Catal. Chem. (2014) 388–389, https://doi.org/10.1016/j.molcata.2013.09.012, 100–105.
[7] R. Tomer, P. Biswas, Optimization of reaction parameters by using response surface methodology (RSM) for the selective dehydration of glucose to 5-hydroxymethylfurfural (5-HMF), a valuable platform chemical over a mesoporous TiO2 catalyst in dimethylsulfoxide (DMSO) medium, Catal. Today 404 (2022) 201–218, https://doi.org/10.1016/j.cattod.2022.03.019.
[8] F. Shahangi, A.N. Chermahini, M. Saraji, Dehydration of fructose and glucose to 5-hydroxymethylfurfural over Al-KCC-1 silica, J. Energy Chem. 27 (2018) 769–780, https://doi.org/10.1016/j.jechem.2017.06.004.
[9] L. Hu, G. Zhao, X. Tang, Z. Wu, J. Xu, L. Lin, S. Liu, Catalytic conversion of carbohydrates into 5-hydroxymethylfurfural over cellulose-derived carbonaceous catalyst in ionic liquid, Bioresour. Technol. 148 (2013) 501–507, https://doi.org/10.1016/j.biortech.2013.09.016.
[10] N.V. Gromov, T.B. Medvedeva, O.P. Taran, A.V. Bukhtiyarov, C. Aymonier, I. P. Prosvirin, V.N. Parmon, Hydrothermal solubilization–hydrolysis–dehydration of cellulose to glucose and 5-Hydroxymethylfurfural over solid acid carbon catalysts, Top. Catal. 61 (2018) 1912–1927, https://doi.org/10.1007/s11244-018-1049-4.
[11] Z. Cao, Z. Fan, Y. Chen, M. Li, T. Shen, C. Zhu, H. Ying, Efficient preparation of 5-hydroxymethylfurfural from cellulose in a biphasic system over hafnyl phosphates, Appl. Catal., B 244 (2019) 170–177, https://doi.org/10.1016/j.apcatb.2018.11.019.
[12] G. Liu, Y. Xie, C. Wei, C. Liu, F. Song, X. Sun, Y. Zhang, H. Cui, Synergistic catalysis of species in molten salt hydrate for conversion of cellulose to 5-hydroxymethylfurfural, Biomass Bioenergy 158 (2022) 106363, https://doi.org/10.1016/J.BIOMBIOE.2022.106363.
[13] R. Tomer, P. Biswas, Dehydration of glucose/fructose to 5-hydroxymethylfurfural (5-HMF) over an easily recyclable sulfated titania (SO42-/TiO2) catalyst, New J. Chem. 44 (2020) 20734–20750, https://doi.org/10.1039/d0nj04151c.
[14] Y. Te Liao, B.M. Matsagar, K.C.W. Wu, Metal-Organic Framework (MOF)-derived effective solid catalysts for valorization of lignocellulosic biomass, ACS Sustain. Chem. Eng. 6 (2018) 13628–13643, https://doi.org/10.1021/acssuschemeng.8b03683.
[15] Y. Zhang, W. Guan, H. Song, Y. Wei, P. Jin, B. Li, C. Yan, J. Pan, Y. Yan, Coupled acid and base UiO-66-type MOFs supported on g-C3N4 as a bi-functional catalyst for one-pot production of 5-HMF from glucose, Microporous Mesoporous Mater. 305 (2020) 110328, https://doi.org/10.1016/j.micromeso.2020.110328.
[16] L. Hu, Z. Wu, J. Xu, Y. Sun, L. Lin, S. Liu, Zeolite-promoted transformation of glucose into 5-hydroxymethylfurfural in ionic liquid, Chem. Eng. J. 244 (2014) 137–144, https://doi.org/10.1016/j.cej.2014.01.057.
[17] N.R. Peela, S.K. Yedla, B. Velaga, A. Kumar, A.K. Golder, Choline chloride functionalized zeolites for the conversion of biomass derivatives to 5-hydroxymethylfurfural, Appl. Catal. Gen. 580 (2019) 59–70, https://doi.org/10.1016/j.apcata.2019.05.005.
[18] N.A.S. Ramli, N.A.S. Amin, Fe/HY zeolite as an effective catalyst for levulinic acid production from glucose: characterization and catalytic performance, Appl. Catal., B 163 (2015) 487–498, https://doi.org/10.1016/j.apcatb.2014.08.031.
[19] S. Yan, L. Gan, K. Wang, K. Sun, Cost-effective bifunctional lignin-derived carbon supported tin oxide with efficient production of 5-hydroxymethylfurfural from glucose, Chin. J. Chem. Eng. 74 (2024) 154–164, https://doi.org/10.1016/j.cjche.2024.07.002.
[20] P.M. Ganje, S.A. Jabasingh, S.K. Kassahun, H. Kim, Sulfonated graphitic carbon catalyst derived from coffee waste: a sustainable valorization approach for highly efficient production of 5-hydroxymethylfurfural (5-HMF) from fructose, J. Environ. Chem. Eng. 12 (2024) 113639, https://doi.org/10.1016/j.jece.2024.113639.
[21] X. Li, K. Peng, Q. Xia, X. Liu, Y. Wang, Efficient conversion of cellulose into 5-hydroxymethylfurfural over niobia/carbon composites, Chem. Eng. J. 332 (2018) 528–536, https://doi.org/10.1016/j.cej.2017.06.105.
[22] Q. Wu, G. Zhang, M. Gao, S. Cao, L. Li, S. Liu, C. Xie, L. Huang, S. Yu, A. J. Ragauskas, Clean production of 5-hydroxymethylfurfural from cellulose using a hydrothermal/biomass-based carbon catalyst, J. Clean. Prod. 213 (2019) 1096–1102, https://doi.org/10.1016/j.jclepro.2018.12.276.

[23] L.J. Konwar, J. Boro, D. Deka, Review on latest developments in biodiesel production using carbon-based catalysts, Renew. Sustain. Energy Rev. 29 (2014) 546–564, https://doi.org/10.1016/J.RSER.2013.09.003.
[24] P. Veerakumar, P. Thanasekaran, T. Subburaj, K.-C. Lin, A metal-free carbon-based catalyst: an overview and directions for future, Research, C 4 (2018) 54, https://doi.org/10.3390/C4040054. Page 54 4 (2018).
[25] L. Yan, N. Liu, Y. Wang, H. Machida, X. Qi, Production of 5-hydroxymethylfurfural from corn stalk catalyzed by corn stalk-derived carbonaceous solid acid catalyst, Bioresour. Technol. 173 (2014) 462–466, https://doi.org/10.1016/j.biortech.2014.09.148.
[26] B. Das, K. Mohanty, Sulfonic acid-functionalized carbon coated red mud as an efficient catalyst for the direct production of 5-HMF from D-glucose under microwave irradiation, Appl. Catal. Gen. 622 (2021), https://doi.org/10.1016/j.apcata.2021.118237.
[27] X. Lyu, H. Li, H. Xiang, Y. Mu, N. Ji, X. Lu, X. Fan, X. Gao, Energy efficient production of 5-hydroxymethylfurfural (5-HMF) over surface functionalized carbon superstructures under microwave irradiation, Chem. Eng. J. 428 (2022) 131143, https://doi.org/10.1016/j.cej.2021.131143.
[28] C. Tempelman, U. Jacobs, J. Herselman, R. van Driel, F. Schraa, J. Versijde, T. van Waversveld, Y. Yagci, M. Barg, F. Smits, F. Kuijpers, K. Lamers, T. Remijn, V. Degirmenci, Waste apple biomass conversion to 5-HMF over tin doped sulfonated activated carbon as a catalyst, Biomass Bioenergy 168 (2023) 106661, https://doi.org/10.1016/j.biombioe.2022.106661.
[29] T. Tongtummachat, K. Thongkan, W. Chuphueak, A. Jaree, N. Akkarawatkhoosith, Efficient continuous-flow separation and purification processes of 5-hydroxymethylfurfural, Chem. Eng. J. Adv. 20 (2024) 100641, https://doi.org/10.1016/J.CEJA.2024.100641.
[30] J. Slak, B. Pomeroy, A. Kostyniuk, M. Grilc, B. Likozar, A review of bio-refining process intensification in catalytic conversion reactions, separations and purifications of hydroxymethylfurfural (HMF) and furfural, Chem. Eng. J. 429 (2022) 132325, https://doi.org/10.1016/J.CEJ.2021.132325.
[31] S. Carlier, S. Hermans, Highly efficient and recyclable catalysts for cellobiose hydrolysis: systematic comparison of carbon nanomaterials functionalized with benzyl sulfonic acids, Front. Chem. 8 (2020), https://doi.org/10.3389/fchem.2020.00347.
[32] A. Tonelli, R. Tomer, A. Morena, L. Fusaro, C. Aprile, S. Hermans, Carbon-based bifunctional Lewis/Brønsted acid catalysts for 5-HMF production from cellobiose, ChemCatChem (2025) e202500070, https://doi.org/10.1002/CCTC.202500070.
[33] Z. Tang, J. Su, Direct conversion of cellulose to 5-hydroxymethylfurfural (HMF) using an efficient and inexpensive boehmite catalyst, Carbohydr. Res. 481 (2019) 52–59, https://doi.org/10.1016/j.carres.2019.06.010.
[34] S.L. Goertzen, K.D. Thériault, A.M. Oickle, A.C. Tarasuk, H.A. Andreas, Standardization of the Boehm titration. Part I. CO2 expulsion and endpoint determination, Carbon N Y 48 (2010) 1252–1261, https://doi.org/10.1016/j.carbon.2009.11.050.
[35] A.M. Oickle, S.L. Goertzen, K.R. Hopper, Y.O. Abdalla, H.A. Andreas, Standardization of the Boehm titration: part II. Method of agitation, effect of filtering and dilute titrant, Carbon N Y 48 (2010) 3313–3322, https://doi.org/10.1016/j.carbon.2010.05.004.
[36] X. Yi, Y.K. Peng, W. Chen, Z. Liu, A. Zheng, Surface fingerprinting of faceted metal oxides and porous zeolite catalysts by probe-assisted solid-state NMR approaches, Acc. Chem. Res. 54 (2021) 2421–2433, https://doi.org/10.1021/ACS.ACCOUNTS.1C00069.
[37] M. Hunger, W. Wang, Characterization of solid catalysts in the functioning state by nuclear magnetic resonance spectroscopy, Adv. Catal. 50 (2006) 149–225, https://doi.org/10.1016/S0360-0564(06)50004-5.
[38] L. Soumoy, A. Maertens, A. Morena, L. Fusaro, M. Armandi, S. Fiorilli, D. P. Debecker, C. Aprile, Low dimensional Zr-based catalysts for the effective upgrading of ethyl levulinate to γ-valerolactone, Mater. Today Chem. 40 (2024) 102189, https://doi.org/10.1016/J.MTCHEM.2024.102189.
[39] A.P. Hammersley, FIT2D: a multi-purpose Data Reduction, Analysis and Visualization Program, 49, Urn:Issn, 2016, pp. 1600–5767, https://doi.org/10.1107/S1600576716000455, 646–652.
[40] S. Carlier, W. Baaziz, O. Ersen, S. Hermans, Synergy between sulfonic functions and Ru nanoparticles supported on activated carbon for the valorization of cellulose into sorbitol, Catalysts 13 (2023) 963, https://doi.org/10.3390/catal13060963.
[41] A. Zheng, S. Bin Liu, F. Deng, 31P NMR chemical shifts of phosphorus probes as reliable and practical acidity scales for solid and liquid catalysts, Chem. Rev. 117 (2017) 12475–12531, https://doi.org/10.1021/ACS.CHEMREV.7B00289/ASSET/IMAGES/LARGE/CR-2017-00289P_0042. JPEG.
[42] X. Yi, H.H. Ko, F. Deng, S. Bin Liu, A. Zheng, Solid-state 31P NMR mapping of active centers and relevant spatial correlations in solid acid catalysts, Nat. Protoc. 15 (10 15) (2020) 3527–3555, https://doi.org/10.1038/s41596-020-0385-6, 2020.
[43] C. Bornes, M. Fischer, J.A. Amelse, C.F.G.C. Geraldes, J. Rocha, L. Mafra, What is being measured with P-Bearing NMR probe molecules adsorbed on zeolites? J. Am. Chem. Soc. 143 (2021) 13616–13623, https://doi.org/10.1021/JACS.1C05014/ASSET/IMAGES/LARGE/JA1C05014_0005.JPEG.
[44] S. Hermans, C. Diverchy, O. Demoulin, V. Dubois, E.M. Gaigneaux, M. Devillers, Nanostructured Pd/C catalysts prepared by grafting of model carboxylate complexes onto functionalized carbon, J. Catal. 243 (2006) 239–251, https://doi.org/10.1016/J.JCAT.2006.07.019.
[45] Y. Yang, C.W. Hu, M.M. Abu-Omar, Conversion of carbohydrates and lignocellulosic biomass into 5-hydroxymethylfurfural using AlCl 3·6H 2O catalyst in a biphasic solvent system, Green Chem. 14 (2012) 509–513, https://doi.org/10.1039/c1gc15972k.
[46] A. Rezayan, Y. Zhang, B. Li, C.C. Xu, Catalytic conversion of cellulose to 5-Hydroxymethylfurfural: Advancements in heterogeneous catalysts and cutting-edge hydrolysis strategies, ChemCatChem 15 (2023) e202300973, https://doi.org/10.1002/CCTC.202300973.
[47] R.S. Assary, P.C. Redfern, J.R. Hammond, J. Greeley, L.A. Curtiss, Computational studies of the thermochemistry for conversion of glucose to levulinic acid, J. Phys. Chem. B 114 (2010) 9002–9009, https://doi.org/10.1021/jp101418f.
[48] V. Choudhary, R.I. Burnett, D.G. Vlachos, S.I. Sandler, Dehydration of glucose to 5-(Hydroxymethyl)furfural and anhydroglucose: thermodynamic insights, J. Phys. Chem. C 116 (2012) 5116–5120, https://doi.org/10.1021/jp2113895.
[49] F. Parveen, S. Upadhyayula, Thermochemical property predictions in biomass transformation to fuel components and value-added chemicals, New Energy Exploit. Appl. 1 (2022), https://doi.org/10.54963/neea.v1i3.70.
[50] W. Guo, H.J. Heeres, J. Yue, Continuous synthesis of 5-hydroxymethylfurfural from glucose using a combination of AlCl3 and HCl as catalyst in a biphasic slug flow capillary microreactor, Chem. Eng. J. 381 (2020) 122754, https://doi.org/10.1016/j.cej.2019.122754.
[51] Y. Yang, C. Hu, M.M. Abu-Omar, The effect of hydrochloric acid on the conversion of glucose to 5-hydroxymethylfurfural in AlCl3-H2O/THF biphasic medium, J. Mol. Catal. Chem. 376 (2013) 98–102, https://doi.org/10.1016/j.molcata.2013.04.016.
[52] R. Tomer, P. Biswas, Dehydration of glucose over sulfate impregnated ZnO (hexagonal-monoclinic) catalyst in dimethyl sulfoxide (DMSO) medium: production, separation, and purification of 5-hydroxymethylfurfural (5-HMF) with high purity, Catal. Today 404 (2022) 219–228, https://doi.org/10.1016/j.cattod.2022.02.009.
[53] D. Gupta, E. Ahmad, K.K. Pant, B. Saha, Efficient utilization of potash alum as a green catalyst for production of furfural, 5-hydroxymethylfurfural and levulinic acid from mono-sugars, RSC Adv. 7 (2017) 41973–41979, https://doi.org/10.1039/c7ra07147g.
[54] Y. Román-Leshkov, J.A. Dumesic, Solvent effects on fructose dehydration to 5-Hydroxymethylfurfural in biphasic systems saturated with inorganic salts, Top. Catal. 52 (2009) 297–303, https://doi.org/10.1007/s11244-008-9166-0.
[55] H. Kimura, K. Yoshida, Y. Uosaki, M. Nakahara, Effect of water content on conversion of D-cellobiose into 5-hydroxymethyl-2-furaldehyde in a dimethyl sulfoxide-water mixture, J. Phys. Chem. A 117 (2013) 10987–10996, https://doi.org/10.1021/jp407801u.
[56] A. Bhalkikar, Z.C. Gernhart, C.L. Cheung, Recyclable magnetite nanoparticle catalyst for one-pot conversion of cellobiose to 5-Hydroxymethylfurfural in water, J. Nanomater. 2015 (2015), https://doi.org/10.1155/2015/264037.
[57] Y.L. Song, Y.H. Qu, C.P. Huang, L.H. Ge, Y.X. Li, B.H. Chen, Single-step conversion of cellobiose to 5-Hydroxymethylfurfural (5-HMF) catalyzed by poly ionic liquid, Adv. Mater. Res. 1004–1005 (2014) 885–890, https://doi.org/10.4028/WWW.SCIENTIFIC.NET/AMR.1004-1005.885.
[58] P. Wrigstedt, J. Keskiväli, T. Repo, Microwave-enhanced aqueous biphasic dehydration of carbohydrates to 5-hydroxymethylfurfural, RSC Adv. 6 (2016) 18973–18979, https://doi.org/10.1039/C5RA25564C.
[59] F. Parveen, S. Upadhyayula, Efficient conversion of glucose to HMF using organocatalysts with dual acidic and basic functionalities - a mechanistic and experimental study, Fuel Process. Technol. 162 (2017) 30–36, https://doi.org/10.1016/j.fuproc.2017.03.021.
[60] W. Guo, H.J. Heeres, J. Yue, Continuous synthesis of 5-hydroxymethylfurfural from glucose using a combination of AlCl3 and HCl as catalyst in a biphasic slug flow capillary microreactor, Chem. Eng. J. 381 (2020), https://doi.org/10.1016/j.cej.2019.122754.